kW pulsed nanosecond TDFL with direct modulation

Clément Romano*[abc], Yves Jaouën[b], Robert E. Tench[a], Jean-Marc Delavaux[a]

[a]Cybel LLC, 1195 Pennsylvania Avenue, Bethlehem, PA USA 18018; [b]Institut Télécom/Télécom ParisTech, 46 Rue Barrault, 75013 Paris, France; [c]Fraunhofer IOSB, Gutleuthausstr. 1, 76275 Ettlingen, Germany

(At the time of this work, Clément Romano was with a & b, and is now with c)

*clement.romano@iosb.fraunhofer.de, www.cybel-llc.com

ABSTRACT

We present a kW level pulsed laser based on a master oscillator power amplifier (MOPA) configuration. The directly modulated single frequency laser at 1952 nm was pulsed in the nanosecond regime with a repetition rate frequency from 10 kHz to 2 MHz. The MOPA topology was based on a two stage amplifier using single clad Thulium-doped fiber: it consisted of a pre-amplifier stage followed by a booster stage. We investigated the performance of this pulsed laser for two different TDFs with different saturating energies in the booster stage. The direct modulation allowed us to demonstrate more than 1 kW of output peak power over pulse repetition frequencies from 10 kHz to 500 kHz. For a pulse duration of 21 ns, we measured output energy of 13 µJ and 29 µJ for booster fiber saturating energies of 15 µJ and 30 µJ, respectively.

Keywords: Pulsed, nanosecond, direct modulation, MOPA, Thulium, 2 microns.

1. INTRODUCTION

Pulsed laser sources in the 2 µm region have attracted much attention for their applications in LIDAR, atmospheric sensing, pumping OPOs, and material processing. Pulsed Thulium-doped fiber lasers (TDFL) operating in the nanosecond regime (<100 ns) have been demonstrated using gain switched cavities, Q-switched cavities, external modulation, or direct modulation. So far, the direct modulation of a semiconductor laser has attracted little attention, except for the publications by H. Shi et al. [1,2] who have reported a MOPA system delivering an average power greater than 100 watts. Although single-frequency lasers at 2 µm have made significant progress, their output power remains moderate, between 1 and 10 mW. This limited output power represents a challenge in pulse mode where the average power is reduced by the duty cycle (e.g. 20 to 30 dB), making the amplification harder to achieve. However, the benefit of a MOPA approach with direct modulation of the seed laser is a cost effective solution with a large flexibility in term of pulse parameters, such as: pulse shape, pulse width (PW), pulse repetition frequency (PRF), and signal wavelength.

Here we report the evaluation of a two stage MOPA pulsed laser delivering more than 1 kW of output peak power over repetition rates from 10 kHz to 500 kHz with pulse widths from 21 ns to 6 ns. This two stage TDFL was based on a pre-amplifier delivering high signal gain followed by a booster stage providing high output peak power. We first describe the pulsed performance of the pre-amplifier, and then contrast the performance of a two stage amplifier using two different single clad Thulium-doped fiber (TDF) with different saturating energy values.

2. EXPERIMENTAL TDFL SETUP

The pulsed MOPA used is shown in Figure 1. This MOPA seed is a single frequency semiconductor laser at 1952 nm whose current is pulsed. The seed is then followed by a pre-amplifier stage and a booster stage.
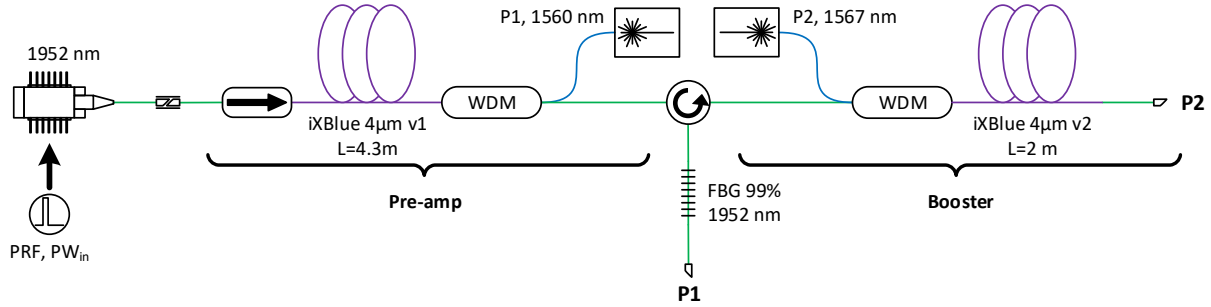
Figure 1: Topology of our pulsed two stage single clad TDFL.

In the CW regime, the seed laser delivers 2.6 mW at 1952 nm. In a pulsed regime, the combined bandwidth of the laser and the driver allows us to generate pulse widths between 6 ns and 21 ns with repetition frequencies from 10 kHz to 2 MHz. As an example, with a pulse width of 21 ns, the seed laser delivers an average power of -10.7 dBm for a PRF=2 MHz and –33.9 dBm for a PRF=10 kHz. Figure 2 shows the normalized output pulse shapes from the semiconductor laser for pulse width of 6, 14, and 21 ns. We can observe the presence of a gain switched pulse of the semiconductor cavity at the beginning of all three pulses. The pulse shapes were recorded with a 12.5 GHz photodiode mounted on a 30 GHz oscilloscope.
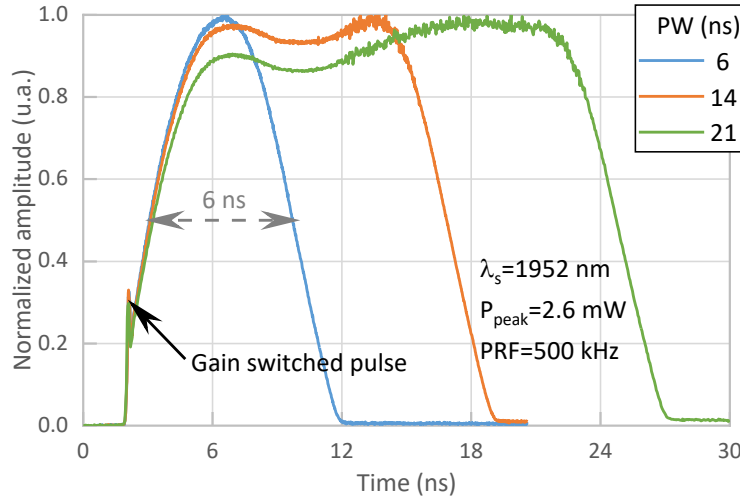

Figure 2: Output pulse shape for three pulse widths from the 1952 nm single frequency seed laser.

The pre-amplifier was designed based on a previous CW study [3], and it is made of a 4.3 m long iXBlue 4 μm v1 Thulium-doped fiber counter-pumped by a 1560 nm fiber laser. The counter-pumping topology was chosen because it provided a higher signal gain than the co-pumping configuration. A mid-stage 1 nm FBG filtered the ASE from the pre-amplifier output to prevent saturation of the booster stage by the large ASE level from the pre-amplifier output. Two topologies were investigated for the booster stage, both designed using a CW study [4]. The first booster stage configuration uses 2 m of iXBlue 4μm v2, while the second booster configuration used 1.2 m of iXBlue 5μm. The two topologies investigated in the booster stage were based on a co-pumped configuration. This allowed to decrease the output signal loss of the amplifier and also decreased the length of output passive fiber, in order to raise the threshold of the onset of non-linearities (i.e. Brillouin, four wave mixing, …). All the pumps of our TDFL were powered in a CW regime.

The characteristics of the different fibers used in this pulsed TDFL are summarized in Table 1, where $\alpha(\lambda)$ is the absorption parameter and $g^*(\lambda)$ is the gain parameter. The fundamental parameters were measured previously for these fibers [5]. The parameters listed are needed to calculate the energy saturation (E_{sat}) [6] at the signal wavelength of 1952 nm. The saturating energy (defined through Equation (1)) is a figure of merit used in the comparison of different fibers. A large saturating energy allows high output energy pulses before a pulse is subject to gain depletion, which results in a change of pulse shape. We note that two 4 μm fibers have comparable saturating energy at the signal wavelength and so should provide

comparable pulse output. The last one, the 5µm, should provide the highest output energy out of the three fibers. The table also gives the maximum measured CW optical slope efficiency ($\eta_{o\text{-}o}$) using a 1567 nm fiber laser pump from our previous study [4].

Parameter	iXBlue single clad Thulium-doped fiber		
Reference	SCF 4µm v1	SCF 4µm v2	SCF 5µm
Core diameter, $2a_{core}$ (µm)	4	4.5	5.3
Numerical aperture, NA (u.a.)	0.27	0.26	0.17
Optical efficiency, $\eta_{o\text{-}o}$ (%)	57	70	53
Doping level, N (x10^{25} m^{-3})	12.3	7.1	25.6
α @ λ_s=1952 nm (dB.m^{-1})	1.55	1.12	4
g^* @ λ_s=1952 nm (dB.m^{-1})	43.8	31.6	80.1
E_{sat} @ λ_s=1952 nm (µJ)	15.1	15.2	29.7

Table 1: Energy saturation and characteristics of three different Thulium-doped fibers used in our pulsed TDFL.

$$E_{sat}(\lambda) = \frac{h.c.\pi.a_{core}^2}{(\alpha(\lambda) + g^*(\lambda))\lambda} \tag{1}$$

3. PRE-AMPLIFIER PERFORMANCE

To test the performance of the pre-amplifier, we monitor the output pulses on port P1 of the setup shown in Figure 1. To perform our measurements, we detuned the seed to an operating wavelength of λ_s=1951 nm, so that its wavelength was out of the reflection bandwidth of the FBG, which was centered at 1952 nm.

In a CW mode, this pre-amplifier delivered small signal gain up to 38 dB for an input power P_{in}=-20 dBm and a pump power P_{p1}=1 W. Figure 3 shows the signal gain versus the pump power for different pulse repetition frequencies. More than 35 dB of gain is achieved, limited by the self lasing occuring in between pulses. We observed a decrease of the gain with an increase of the PRF, clearly noticeable for PRF=2 MHz.
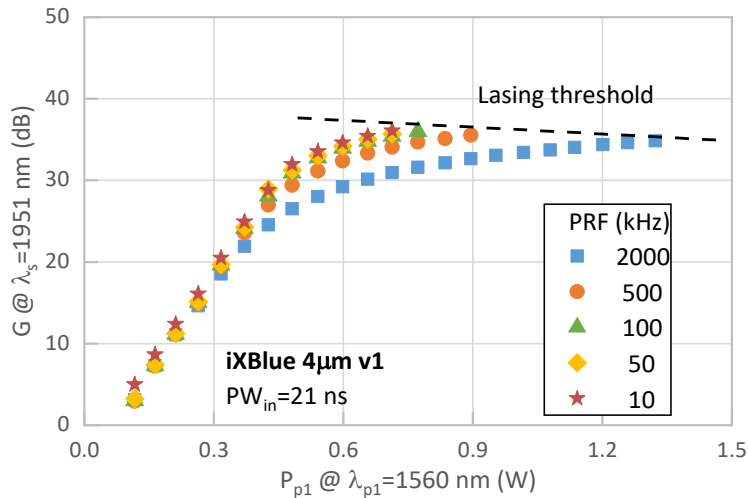

Figure 3: Pre-amplifier signal gain versus pump power for different repetition rate.

The output pulse shape is shown in Figure 4 for a PRF of 500 kHz, a pulse width of 21 ns with a pump power of 0.7 W. We noted that the pulse shape is similar to the pulse shown earlier in Figure 2. For comparison, we have included in Figure

4 the pulse shape calculated using the Frantz-Nodvik approach [6]. We note a good agreement with the pulse shape and a slightly lower amplitude for theory compared to experiment. Overall the amplified pulse did not suffer from gain depletion regime.
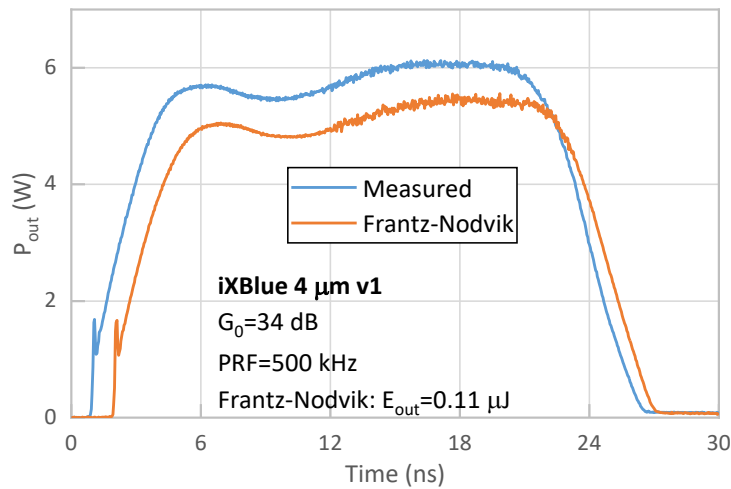

Figure 4: Output pulse shape from the pre-amplifier.

Using the pulse shapes at the different operating conditions, the peak power was derived and is plotted in Figure 5 versus the frequency for the different input pulse widths. We observed an exponential decrease of the peak power with the frequency increasing starting with a maximum of ≈9 W at 10 kHz. For an input pulse width of 21 ns, the measured peak power of 9 W at 10 kHz corresponded to an output energy of 185 nJ. For a PRF of 2 MHz the peak power decreases as the pulse frequency increases. At low repetition rates, the ASE dominates the output spectrum and that could explain why the peak power for the 7 ns pulse width is lower than the 21 ns pulse width. Nevertheless such high peak power will allow the pulse to saturate the booster stage and extract the power.
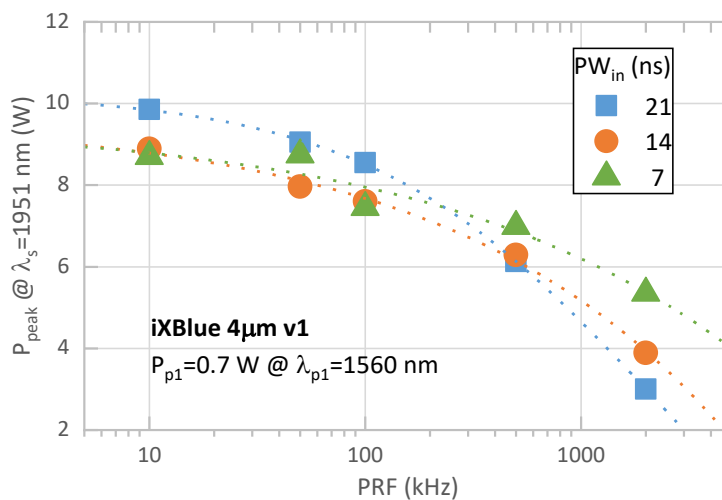

Figure 5: Peak power versus pulse repetition rate for different input pulse width.

Figure 6 illustrates the evolution of the normalized output spectrum of the pre-amplifier versus PRF of an input pulse width of 21 ns. Over the wavelength range from 1700 nm to 2100 nm, we observe that the amount of ASE increases with a decrease in PRF value. The optical signal to noise ratio (OSNR) follows the same trend. Figure 7 shows the ratio of output signal power to total output power ($P_{out}(\lambda_s)/P_{out}$) in a 500 nm bandwidth versus PRF for input pulse widths of 6, 14, and 21 ns. For a same PRF, a decrease in pulse width yields a decrease in the $P_{out}(\lambda_s)/P_{out}$ ratio, equivalent to an increase in ASE power. This clearly indicates that an ASE filter between the pre-amplifier and the booster stage is required to prevent out

of band ASE power from saturating the booster stage. Therefore, we inserted an ASE filter with a 1 nm bandwidth between the preamplifier and booster. The output ASE entering the booster stage was significantly reduced and could not be observed 60 dB below the signal within the observation range from 1700 nm to 2100 nm.
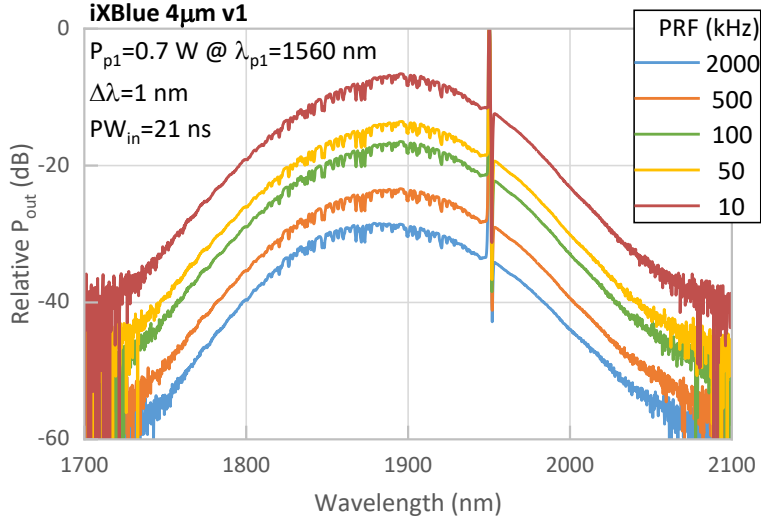

Figure 6: Output spectrum versus the pulse repetition rate for an input pulse width of 21 ns.
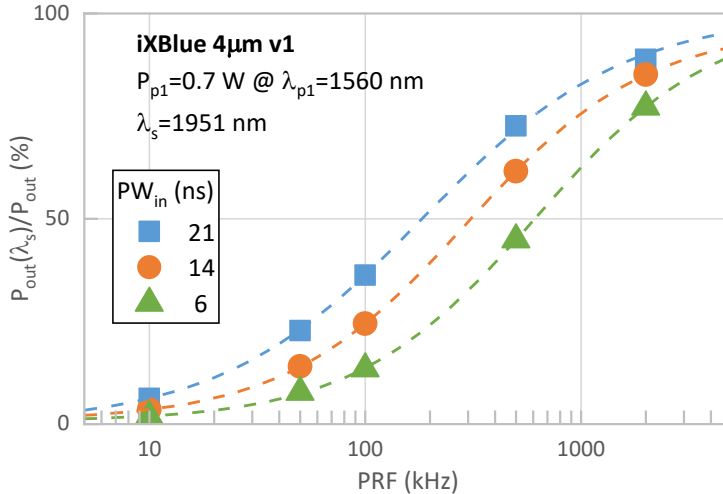

Figure 7: Output spectrum ASE ratio versus the pulse repetition rate for three input pulse width.

4. TWO STAGE PERFORMANCE

With the pre-amplifier pump power set to 0.7 W, we next monitor the output performance of the two stage amplifier on port P2. Three different topologies were investigated in the booster stage: two topologies based on single clad TDF (iXBlue 4 μm v2 L=2 m, and iXBlue 5 μm L=1.2 m) co-pumped with an Er:Yb fiber laser.

We start by comparing the output peak power of the two stage amplifier for an input pulse width of 21 ns as shown in Figure 8 for both configurations. The pulse shape was taken in account in the calculation of the peak power. We observe that for both configurations we were able to deliver an output peak power greater than 1 kW for different pulse repetition frequency. At low PRF (<500 kHz), both configurations were limited by the onset of lasing on top of the ASE in between pulses. The iXBlue 5μm delivered up to 2.7 kW at 10 and 50 kHz, while the iXBlue 4μm v2 delivered up to 1.2 kW at 100 kHz. We note that at 500 kHz only the iXBlue 4μm v2 can provided more than 1 kW of output peak power. One way to overcome the onset of lasing limitation in both amplifiers would be to modulate the pump power, switching it off after the

pulse and back on before the pulse to load the active fiber, allowing us to extract higher energies. These measured peak powers correspond to a maximum output energy of 13 µJ for the iXBlue 4µm v2 configuration and 29 µJ for the iXBlue 5µm configuration.
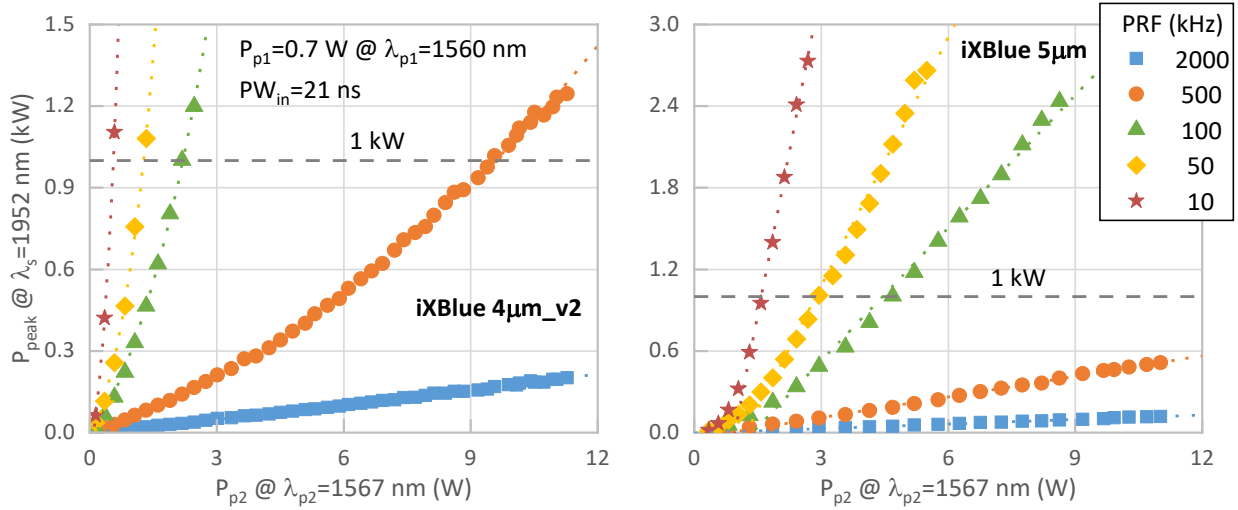

Figure 8: Output peak power as a function of the pump power for the iXBlue 4um_v2 (left) and the iXBlue 5um (right).

We then focused on a PRF of 500 kHz and an input pulse width of 21 ns. The pulse shapes were recorded and the output pulse shapes are displayed for three different signal gain levels with their respective Frantz-Nodvik simulation. Figure 9 shows the evolution of the pulse shape with the pump power increasing. As the pump increases, we observe a distortion of the pulse shape with a gain distributed mainly toward the beginning of the pulse. Comparing the output pulse shape from the two single clad configuration we note that the output pulse shape from the iXBlue 5µm configuration is less distorted than the ones from the iXBlue 4µm v2 at comparable gain G_0, which confirms that the iXBlue 5µm has a larger saturating energy than the iXBlue 4µm v2. The distortion effect is the result of the gain depletion in the amplifier. Using the Frantz-Nodvik model this can be predicted. The Frantz-Nodvik model applied on the output pulses of the pre-amplifier and the booster stage gave us the dashed curves for the three different gain level studied. We note a strong difference between the measured pulse shape and the shape modeled by the Frantz-Nodvik equation for both single clad TDF configurations and different gain level.

One way to prevent this gain depletion is to use a pre-shaped pulse coming out of the semiconductor laser diode. This has been demonstrated for 100 ns pulses in TDFL based on direct modulation in the paper by H. Shi et al. [2].
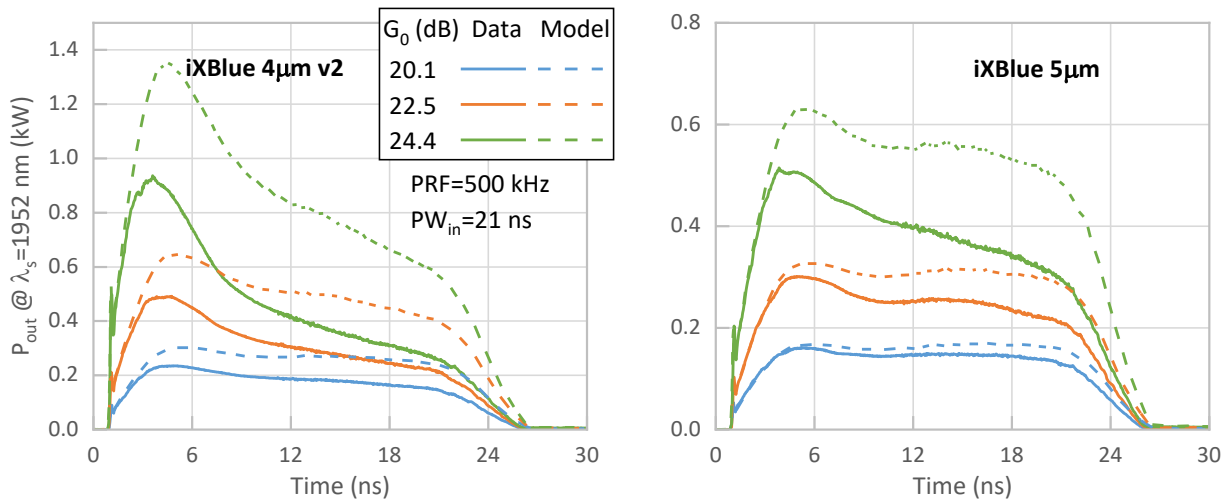

Figure 9: Output pulse shape for for the iXBlue 4um_v2 (left) and the iXBlue 5um (right).

The output pulse width (PW$_{out}$) evolution versus pump power was measured for different input pulse widths and is shown in Figure 10 for the two TDF single clad configurations. We observe that for the iXBlue 4µm v2 configuration, the output pulse width depends on the pump power and the input pulse width: at low pump power the pulse width is independent of the pump power whereas above 6 W of pump power we observe a decrease of the pulse width with an increasing pump power. The pulse width seems to converge towards a value of 5-6 ns. With the iXBlue 5µm configuration, we do not observe a dependence of the output pulse width on the pump power. This confirms the effect difference in gain depletion observed in Figure 9 for the the iXBlue 4µm v2, which has a lower saturation energy than the iXBlue 5µm.
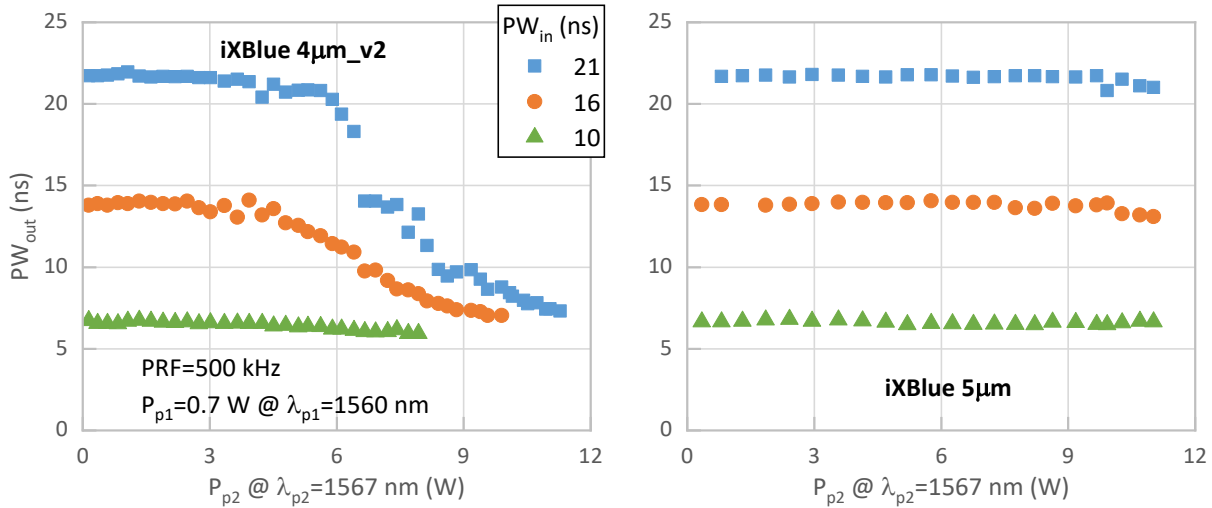

Figure 10: Output pulse width versus output energy for three different input pulse widths for the iXBlue 4um_v2 (left) and the iXBlue 5um (right).

Next, we study the dependence of the performance on the input pulse width. Figure 11 shows the evolution of the pulse peak power with the pump power for three different input pulse widths for both single clad configurations. We observed for both configurations that with a decreasing pulse width, the peak power increases non-linearly. For the iXBlue 5µm configuration, at a pump power of 5.8 W the output peak power is 1.4 kW, 1.8 kW, and 2.5 kW for a pulse width of 21 ns, 14 ns, and 6 ns, respectively.
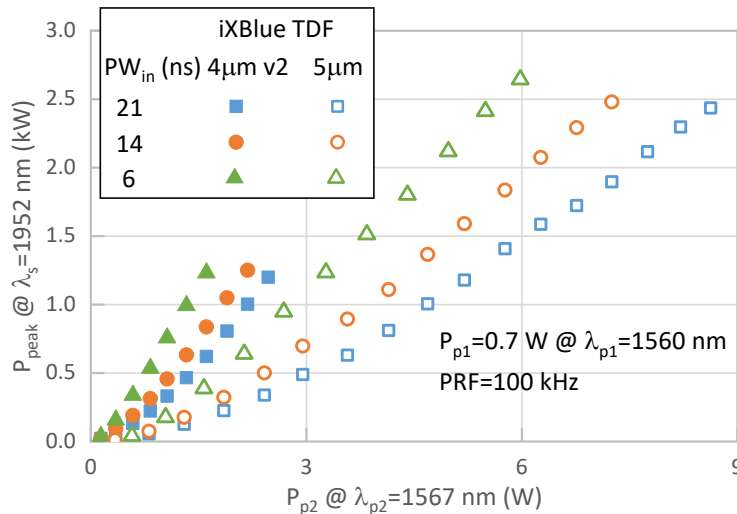

Figure 11: Peak power versus 1567 nm pump power for three different input pulse width.

The normalized output spectrum of the iXBlue 5µm configuration is shown for an output peak power of 2.5 kW for different input pulse width in Figure 12. We observed no significant difference in the output spectra with the different input pulse width. The side lobes on each side of the signal are attributed to the modulation instability (MI) [7] due to the

high peak power combined with the chirp of the semiconductor seed laser. At a wavelength of 1952 nm the dispersion of the Thulium-doped fiber was measured to be -18 $ps^2.nm^{-1}$ [8] which is one of the requirements to have MI. The MI results from four-wave mixing between the signal and the noise, and limits the power amplification as the energy is transferred to the side lobes.

At an output peak power of 2.5 kW, less than 1 % of the energy is in the side lobes. The setup had an output pigtail of 1 m long (Nufern SM1950) to limit the generation of non-linearities. Therefore one way to reduce the MI is to shorten the output pigtail length (e.g. 0.5 m or less).
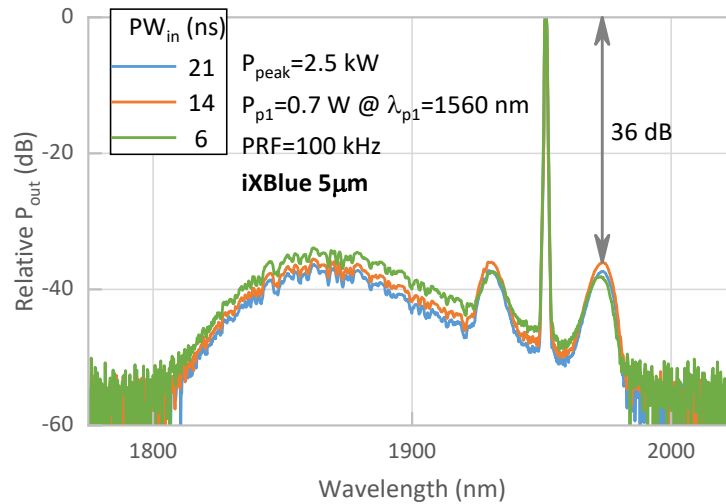

Figure 12: Output spectrum for different 1567 nm pump power.

5. CONCLUSION

We demonstrated two TDFL topologies based on direct modulation of a semiconductor laser diode, operating at 1952 nm, which can deliver more than 1 kW of peak power for three different pulse width (i.e. 6, 14, and 21 ns) and a wide range of pulse repetition frequencies (i.e. 10 to 500 kHz). Our setup was composed of a pre-amplifier followed by a booster stage. The pre-amplifier was designed to deliver high gain to saturate and extract the energy from the booster stage. It delivered output peak powers between 5 and 9 W for pulse repetition frequencies between 2 MHz and 10 kHz, respectively. In the booster stage we investigated two single clad TDFs from iXBlue with different saturating energies. Using the iXBlue 4µm v2 the TDFL delivered up to 13 µJ while with iXBlue 5µm it yielded up to 29 µJ. Through gain depletion of the active fiber, we observed a distortion of the pulse shape, which reduces the output pulse width, for PRF less than 2 MHz for the iXBlue 4µm v2 and less than 500 kHz for the iXBlue 5µm. The maximum output peak powers reached are 1.2 kW and 2.5 kW for the iXBlue 4µm v2 and iXBlue 5µm, respectively.

6. ACKNOWLEDGEMENTS

7. BIBLIOGRAPHY

[1]   H. Shi, J. Liu, K. Liu, F. Tan, P. Wang, 160 W average power single-polarization, nanosecond pulses generation from diode-seeded thulium-doped all fiber MOPA system, in: SPIE Fiber Lasers XII Technol. Syst. Appl., 2015: p. 93441O. doi:10.1117/12.2079343.

[2]   H. Shi, F. Tan, Y. Cao, P. Wang, P. Wang, High-power diode-seeded thulium-doped fiber MOPA incorporating active pulse shaping, Appl. Phys. B. 122 (2016) 269. doi:10.1007/s00340-016-6543-4.

[3]   C. Romano, R.E. Tench, J.-M. Delavaux, 5W 1950nm Brillouin-free efficient single clad TDFA, in: Laser Technol. Def. Secur. XIV, 2018. doi:10.1117/12.2304910.

[4]   C. Romano, R. Tench, J. Delavaux, 8W 1952nm Highly Efficient Brillouin-free Single Clad TDFA, in: ECOC Pap. We2.5, 2018.

[5]   C. Romano, R.E. Tench, J.-M. Delavaux, Y. Jaouen, Characterization of the 3F4–3H6 Transition in Thulium-Doped Silica Fibres and Simulation of a 2μm Single Clad Amplifier, in: 2017 Eur. Conf. Opt. Commun., IEEE, Gothenburg, 2017: pp. 1–3. doi:10.1109/ECOC.2017.8345894.

[6]   L.M. Frantz, J.S. Nodvik, Theory of Pulse Propagation in a Laser Amplifier, J. Appl. Phys. 34 (1963) 2346–2349. doi:10.1063/1.1702744.

[7]   G.P. Agrawal, Nonlinear fiber optics, 2013. doi:10.1016/C2011-0-00045-5.

[8]   S. Kharitonov, A. Billat, C.-S. Brès, Kerr nonlinearity and dispersion characterization of core-pumped thulium-doped fiber at 2 μm, Opt. Lett. 41 (2016) 3173. doi:10.1364/OL.41.003173.